A theoretical study of the effect of *ansa*-bridges on the energy barrier to hydrogen exchange in a series of biscyclopentadienyl tungsten trihydride cations

Jennifer C. Green* and Adrian Scottow

Inorganic Chemistry Laboratory, South Parks Road, Oxford, UK OX1 3QR.
E-mail: Jennifer.Green@chem.ox.ac.uk

Received* (*in Montpellier, France*) *on 17th February 1999, Accepted 6th April 1999

Density functional calculations have been carried out on the structures and pathway for hydrogen exchange of the tungsten trihydride cations, $[W(\eta\text{-}C_5H_5)_2H_3]^+$, **I**, $[W\{(\eta\text{-}C_5H_4)_2SiH_2\}H_3]^+$, **II**, and $[W\{(\eta\text{-}C_5H_4)_2CH_2\}H_3]^+$, **III**, as models for the characterised trihydride cations $[W(\eta\text{-}C_5H_5)_2H_3]^+$, **1**, $[W\{(\eta\text{-}C_5H_4)_2SiMe_2\}H_3]^+$, **2**, and $[W\{(\eta\text{-}C_5H_4)_2CMe_2\}H_3]^+$, **3**. The most significant difference found for the ground state structures is the increase in inter-ring angle in the order **I** < **II** < **III**. The barrier to pairwise exchange of the central and a lateral hydride is found to decrease in the order **I** > **II** > **III**. Also the ease of the in-plane bending motion decreases in the same order. For **III**, a dihydrogen hydride structure is found as an intermediate on the bending pathway. The exchange energy barriers for **II** and **III** of 63 and 51 kJ mol^{-1} are consistent with the large temperature dependent H–H coupling constants previously reported for cations **2** and **3**, which have been attributed to quantum mechanical exchange coupling. The barrier calculated for **I**, of 96 kJ mol^{-1}, lies outside the range wherein such unusual coupling is expected and **1** is reported to have a small temperature independent coupling constant. The relative ease of approach calculated for the two hydrogens is also consistent with the view that the quantum mechanical exchange is facilitated by a short tunnelling path. The underlying reasons for the differences found for the series **I**–**III** are twofold. As the inter-ring angle increases the rings become more tightly bound and the hydrides less tightly bound. The exchange pathway involves reduction of the metal from a d^0 to a d^2 configuration, and the d orbital involved becomes more stable on bending the rings.

A number of transition metal polyhydride systems have been identified for which the ^{1}H NMR spectra, of an AB_x spin system, show large temperature dependent H_A–H_B coupling constants.[1–5] This phenomenon has been explained by the ability of the hydride ligands to undergo quantum mechanical exchange coupling.[6–9]

Various models for the potential energy surface of the exchange between the hydride ligands, and the temperature dependence of the couplings, have been proposed.[10–19] The current understanding of the phenomenon has been well summarised by Sabo-Etienne and Chaudret in their recent review.[5] (*a*) There is a low energy MH_2 bending vibration that allows close approach of the two exchanging hydrogens.[18] (*b*) There is a chemical pathway to exchange initiated by this vibration. In some cases, a coordinated dihydrogen ligand may exist as an energy minimum along this path; however, this is not necessarily the case. (*c*) The barrier to the chemical or classical exchange must lie in the region of 35–70 kJ mol^{-1} for the phenomenon to be detectable by ^{1}H NMR. If the barrier is too high, the quantum exchange couplings are too small to be observed, whereas if the barrier is too small classical exchange leads to signal coalescence. (*d*) There is rotational tunnelling through the barrier. (*e*) The observed temperature dependence of J_{ex} is a consequence of thermal population of excited vibrational states, which inevitably have lower potential energy barriers for tunnelling. Experimental evidence for non-zero values of J_{ex} at 0° K rules out the postulate of the barrier just being a rotational one for a dihydrogen complex, thermally accessible from a ground state hydride structure.[18]

Complexes displaying quantum mechanical exchange couplings include biscyclopentadienyl metal trihydride systems, $[Cp_2MH_3]^{n+}$ [$Cp = (C_5H_{5-x}R_x)$; M = Nb, Ta, $n = 0$; M = Mo, W, $n = 1$],[3,20–24] and the closely related dihydrides, $[Cp_2MH_2L]$ (M = Nb, Ta; L = PR_3, CO, CNR,[25–27] cyclopentadienyl metal trihydride phosphine systems $[CpMH_3L]^{n+}$ (M = Ru, $n = 0$; M = Ir, $n = 1$; L = PR_3)[2,4,7,18,28–31] and the isoelectronic osmium trihydrides $[(C_6H_6)OsH_3(PR_3)_2]^+$,[32] and octahedral polyhydrides such as $OsH_3X(PR_3)_2$ (X = Cl, Br, I, 2,2′-biimidazole, dienes).[33–35]

The values of J_{ex} vary by several orders of magnitude; however, it is generally found in a series of related compounds that the magnitude of the exchange coupling increases as the barrier to the classical thermally activated rearrangement between the A and B hydrides decreases.[18] However, this is not the only criteria as comparison of $\Delta G^{\#}$ with J_{HH} shows.[5] The length of the exchange path also pays an important role in determining the magnitude of quantum mechanical exchange.

By studying related compounds, J_{ex} has been shown to decrease with increased basicity of the co-ligands, increase with charge on an isoelectronic pair and decrease between the second and third transition series.[18] Recently, $J_{H_AH_B}$ was found to vary significantly within a series of compounds where none of these factors were changing.[22,23] The biscyclopentadienyl tungsten trihydride cation, $[W(\eta\text{-}C_5H_5)_2H_3]^+$, **1**, shows normal $J_{H_AH_B}$ values of 8.5 Hz at all temperatures. When the rings are *ansa*-bridged by $SiMe_2$, $[W\{(\eta\text{–}C_5H_4)_2SiMe_2\}H_3]^+$, **2**, and CMe_2, $[W\{(\eta\text{-}C_5H_4)_2CMe_2\}H_3]^+$, **3**, the values are significantly different. **2** has $J_{H_AH_B}$ varying from 8 Hz at −140 °C to 75 Hz at 0 °C while **3** shows more extreme behaviour with $J_{H_AH_B}$ varying from 2900 Hz at −130 °C to 16 000 Hz at −70 °C. The principal change in this series is the inter-ring angle, which increases as the bridge becomes more sterically constraining.

We are concerned with an ongoing investigation of the effect of *ansa*-bridges on the electronic structure of metallocenes.[36] In particular we have studied hydrogen exchange and methane elimination in biscyclopentadienyl tungsten methyl hydrides, with and without *ansa*-bridges, by density functional methods.[37] Camanyes *et al.* have modelled hydrogen exchange coupling in metallocene trihydride systems.[39] They carried out density functional calculations to obtain a potential energy profile for the reaction pathway and then applied a dynamic tunnelling model to calculate values for the exchange coupling constants. A similar approach had been taken previously in estimating the barrier in the $CpIrH_3L$ systems,[39,40] and subsequently applied to the Cp_2MH_2L system[41] and $Cp_2NbH_3 \cdot AlH_3$.[42] This success encouraged us to see whether density functional calculations could illuminate the trends in the barrier to chemical exchange that are indicated by the relative magnitudes of the quantum mechanical exchange couplings found for **1**–**3**. Our aim in this study is to see to what extent the variation of J_{ex} in the series **1-3** can be understood in terms of the changes in electronic structure brought about by the *ansa*-bridges.

Computational methods

All calculations were carried out using the Amsterdam Density Functional (ADF) program system, version 2.3.[43] The electronic configurations of the molecular systems were described by an uncontracted triple-ζ basis set of Slater-type orbitals (STO). Hydrogen, carbon and silicon were given an extra polarisation function: 2p on H, 3d on C and 4d on Si. The cores of the atoms were frozen: C up to 1s, Si up to 2p and W up to 5p. First-order relativistic corrections were made to the cores of all atoms using the Pauli formalism. Energies were calculated using Vosko, Wilk and Nusair's local exchange correlation potentials[44] with non-local exchange corrections by the method of Becke[45] and non-local correlation corrections by that of Perdew.[46,47]

Methodology

Given the relatively large size of the molecules under consideration, we adopted a relatively simple approach to estimate the classical barrier to intra-molecular hydrogen exchange in **1-3**, similar to, but not identical with, that of Camanyes *et al.*[38] The methyl groups on the *ansa*-bridges were replaced by hydrogens to save computational time, so calculations were carried out on the cations **I**, **II** and **III**. The geometries of molecular ion ground state structures, **a** (Fig. 1), were optimised, with an initial assumption of C_{2v} symmetry, with the hydrides lying in the *xz* plane. For **I**, there are two alternative C_{2v} structures; they differ in the orientations of the cyclopentadienyl rings. That with the rings oriented so that two carbons approach each other on bending was found to be the more stable by 18 kJ mol^{-1} and was taken to be the minimum energy structure.

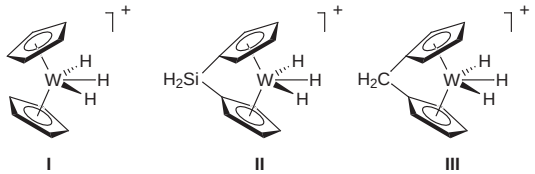

I **II** **III**

The mid-point of the exchange was assumed to be an η^2–H_2 structure with the H–H axis perpendicular to the *xz* plane, **c** (Fig. 1). If the rings are assumed to be eclipsed, this structure possesses a mirror plane, so the minimum energy was found by a full optimisation with the constraint of C_s symmetry. The energy difference between **a** and **c** gives an estimate of the height of the barrier to H exchange.

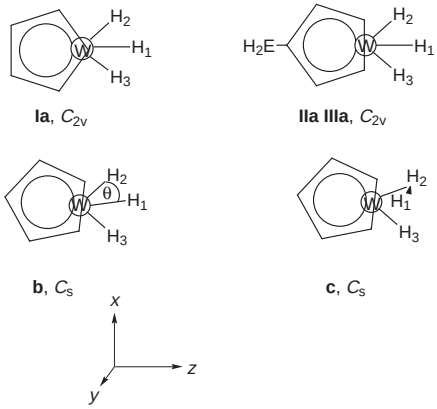

Ia, C_{2v} **IIa IIIa**, C_{2v}

b, C_s **c**, C_s

Fig. 1 Structures and symmetries assumed for the metallocene trihydride cations in the calculations of **a**, the ground states, **b**, the WH_2 bend, and **c**, the mid-point of the H_1–H_2 exchange.

The ease of approach of the exchanging hydrogens within the *xz* plane was modelled by a linear transit run in which C_s symmetry was assumed with all three hydrogens lying in the *xz* plane, **b** (Fig. 1). The H_1–W–H_2 angle was fixed to successive values and the rest of the structure optimised within the C_s symmetry constraint. This gave an estimate of the ease of the initial WH_2 bending vibration, and an impression of the shape of the barrier, which has been shown to be important in the magnitude of the coupling.

Frequency calculations were carried out to test some of the key minima and transition states.

Results

Ground state optimisations

Structural parameters calculated for the minimum energy structures, **a**, of **I**–**III** are given in Table 1. Where structural data is available for **1**–**3** (see Table 1), there is good agreement between the calculated and experimental values. The calculated values for the W–H distances of **I** are similar to those calculated by Camanyes *et al.*;[38] our values were 0.02 Å longer. In their calculation local fivefold symmetry was assumed for the C_5H_5 rings, but in our calculations the ring geometry was allowed to optimise under the C_{2v} symmetry constraint. The Cp_{cent}–W–Cp_{cent} angles found for **I**–**III** were close to those found in related C and Si *ansa*-bridged metallocenes, which lie around 128° and 138°, respectively.[22,23]

A frequency calculation on the ground state structure found for **III** gave an imaginary frequency of 120*i* cm^{-1} of b_1 symmetry. This corresponded to a movement of the central hydrogen, in the *xz* plane, to the side of the W-bridging C vector.

Table 1 Selected calculated structural parameters[a] (Å and °) for **I**, **II**, and **III** (when available, experimental data is given in parentheses)

	Ia[b]	**IIa**	**IIIa**[c]
W–H_1	1.712	1.734	1.739
W–$H_{2,3}$	1.700	1.707	1.715
$H_1 \cdots H_{2,3}$	1.699	1.602	1.650
W–C_{av}	2.354(2.261)	2.353	2.349
W–Cp_{cent}	2.021	2.021	2.014(1.963)
C–C (av)	1.417	1.421	1.420
H_1–W–$H_{2,3}$	58.7	55.5	57.1
α	29(31.8)	48	62
Cp_{cent}–W–Cp_{cent}	150	137	125(127.08)
β	1	23	19

[a] α is the inter-ring angle; β is the angle between the ring plane and the *ipso*-carbon substituent vector; Cp_{cent} denotes the centroid of a C_5 ring. [b] Ref. 48. [c] Ref. 22.

Table 2 Calculated structural parameters (Å and °) for the WH_3 unit of **I**, **II**, and **III** for the ground states **a**, with an H_1–W–H_2 angle of 31°, for **b** and for the mid-point of the exchange reaction, **c**

	Ia	IIa	IIIa	Ib	IIb	IIIb	Ic	IIc	IIIc
W–H_1	1.712	1.734	1.739	1.820	1.819	1.837	1.934	1.956	1.978
W–H_2	1.700	1.707	1.715	1.804	1.792	1.806	1.934	1.956	1.978
W–H_3	1.700	1.707	1.715	1.701	1.715	1.725	1.708	1.711	1.730
$H_1\cdots H_2$	1.699	1.602	1.650	0.969	0.965	0.974	0.836	0.829	0.822
$H_1\cdots H_3$	1.699	1.602	1.650	2.034	1.939	1.946	2.346	2.367	2.397
H_1–W–H_2	60	55	56	31	31	31	25	25	24
α	29	48	62	36	49	63	40	49	63

The structure was re-optimised with no symmetry constraint, and the structure found had an angle of 172° between the W–H_1 vector and the W-bridging carbon vector. The new structure was of the same energy to within 0.01 eV and, apart from the angle mentioned the distances and angles were the same.

The initial impression from inspection of the trends in distance along the series is that there is little variation in the geometry of the WH_3 unit. Close examination suggests that, as the inter-ring angle increases, the metal becomes more closely bound to the ring and possibly less closely bound to the hydrides; however, the calculated variation of distance in the latter case is small.

Mid-point optimisation

Optimisation of the presumed mid-point of the exchange with H_1–H_2 perpendicular to the *xz* plane gave structural data for the WH_3 units shown in Table 2 and energies above the ground state given in Table 3. Variations were found in the metallocene fragment. These were minor except in the case of **Ic** where the inter-ring angle, α, increased to 40° at the mid-point. In the cases of **II** and **III**, the inter-ring angle at the mid-point was similar to that calculated for the minimum energy structure.

The distance between the exchanging hydrogens at the mid-point was found to range from 0.84 Å for **Ic** to 0.82 Å for **IIIc**. This is significantly longer than the value of 0.783 Å calculated in the previous work.[38] The W–H_1 and W–H_2 distances of 1.93 Å found for **I** were, however, the same. A frequency calculation was carried out on **Ic**, which confirmed the structure as a transition state, there being one imaginary frequency of 854*i* cm^{-1} corresponding to rotation of the dihydrogen unit.

The difference in H–H distance calculated by Camanyes *et al.*[38] and that reported here could be due to a number of factors: difference in basis sets, functionals, core treatments, or geometry constraints mentioned above. We have not carried out a systematic investigation as to the origin of the discrepancy as we are more concerned with the trend found for a series of compounds when a consistent theoretical methodology is applied.

The W–H distances were found to increase from **I** to **II** to **III**. This increase was associated with the small decrease in H_1–H_2 distance noted above. Thus, the differences in the WH_3 unit seem more pronounced at the mid-point than in the minimum energy structures.

The energy differences between the minimum energy structures and the mid-points (Table 3) show a decrease from 96 kJ mol^{-1} for **I** to 63 kJ mol^{-1} for **II** to 51 kJ mol^{-1} for **III**. Camanyes *et al.* calculated a value of 119 kJ mol^{-1} (28.49 kcal mol^{-1}) for **I**.[38] Thus, the exchange energy barriers for **II** and **III** are calculated to lie in the 35–70 kJ mol^{-1} region within which quantum mechanical exhange coupling has been found to occur, whereas that for **I** lies outside this range, and no exhange coupling has been observed for this cation.

Table 3 Calculated energies (kJ mol^{-1}) of structures **b** (with θ = 31°) and **c** relative to **a**

	I	II	III
b	30.2	15.0	6.8
c	95.5	62.5	51.3

H_1WH_2 bend

The energies of structures **b** relative to the minimum energy **a** as the H_1–W–H_2 angle, θ, is varied are given in Fig. 2. The ease of distortion increases in the order **I** to **III**. Compound **III** shows a minimum on the energy surface when the angle θ is around 31°. The H_1–H_2 value at this angle is 0.97 Å. The other two compounds show points of inflexion in the energy curve at similar values. The structural details for the WH_3 units at θ = 31° are given in Table 2 and the energies at this point in Table 3.

We tested whether there was a true minimum on the energy surface for **III** at this angle by optimising the structure with no symmetry constraints with the starting parameters from the linear transit run. The minimum found had a H_1–W–H_2 angle of 33°.

Discussion

The calculations are in excellent agreement with the model for quantum mechanical exchange coupling outlined in the introduction. The two key features are the ease of close approach of the exchanging hydrogens so that the tunnelling distance is small and the size of the barrier to classical exchange, which should lie between 35 and 70 kJ mol^{-1} for the phenomenon to be observable by ^1H NMR.

Our calculations on the models **I**, **II** and **III** suggest the energy barrier is too high for **1** where no quantum mechanical exchange coupling is observed, but that for both **2** and **3** the barrier is in the correct range and that it is lower for **3** than **2**.

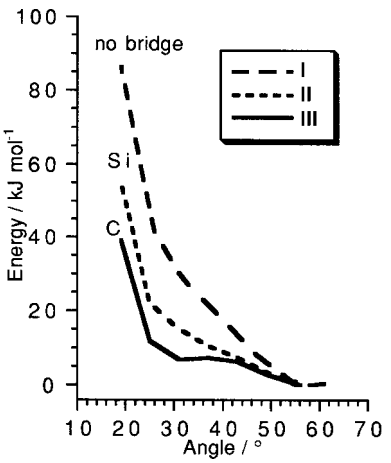

Fig. 2 Energies of the structure **b** relative to the ground state **a** as the H_1–W–H_2 angle, θ, is varied for **I**, **II** and **III**.

Table 4 Selected atom-atom overlap populations and Mulliken charges for **Ia**–**IIIa**

	Ia	IIa	IIIa
Atom-atom overlap population[a]			
W–H_1	0.045	−0.080	−0.137
W–H_2	0.111	0.040	0.023
H_1–H_2	0.080	0.158	0.189
Mulliken charges			
W	1.29	1.37	1.41
H_1	−0.11	−0.18	−0.23
H_2	−0.09	−0.14	−0.17

[a] Off-diagonal elements are not doubled.

As noted in the introduction, J_{ex} is considerably larger for **3** than **2**.

Moreover, for the two exchanging hydrogens to approach within 0.97 Å of one another requires a decreasing amount of energy in the order **1** to **3** so this factor is also consistent with the experimental results. For **III** the dihydrogen intermediate lies only 7 kJ mol^{-1} above the minimum energy state.

As noted above the most obvious difference between the molecules in this series is the steric constraint on the inter-ring angle introduced by the presence of an *ansa*-bridge. The optimised structural distances for the ground state structures indicate that the central hydrogen, H_1, is the most loosely bound. There is also some indication of a lengthening of the W–H bonds as the inter-ring angle increases. An analysis of the atom-atom overlap populations is revealing in this context. These populations give an indication of covalent bond order; they are given for the WH_3 unit in Table 4. The overlap population between the metal and the central hydrogen, H_1, decreases from **Ia** to **IIIa**; indeed, it is negative for **IIa** and **IIIa**. That between the metal and the lateral hydrogens, H_2 and H_3, is larger, also decreases, but remains positive throughout. That between the central and lateral hydrogens increases from **Ia** to **IIIa**. The Mulliken charges, also given in Table 4, indicate an increase in the positive charge on the metal and an increase in negative charge on the hydrogens in the order **Ia** to **IIIa**. This reinforces the picture, obtained from the distance variations, of the central hydrogen being the most weakly bound and the covalent bonding between the metal and the hydrogens decreasing with increasing inter-ring angle. It is also consistent with the slightly distorted minimum energy structure found for **III**.

The underlying reason for this is apparent from an orbital analysis of the effect of bending of the metallocene unit on the frontier orbitals.[36] The frontier orbitals are represented in Fig. 3, superimposed on a plan of the trihydride structure. The orbital best oriented to bind the central hydrogen is the $4a_1$ orbital, but this is the orbital that rises steeply in energy with increasing inter-ring angle. The metal $d(z^2 - y^2)$ orbital becomes involved in bonding to the cyclopentadienyl π orbitals as the rings are bent. The $4a_1$ orbital is the antibonding counterpart of this bonding interaction. With a large inter-ring angle it lies too high in energy to bond effectively. The $2b_1$ orbital rises in energy on bending for similar reasons, but the rise is not so great. The $3a_1$ orbital, $d(x^2)$ in character, in contrast is effectively non-bonding with respect to the cyclopentadienyl rings and drops in energy on bending.

Formation of the W(η²–H_2)H transition state, **c**, from the WH_3 ground state, **a**, constitutes a formal reduction of the tungsten from VI to IV with its configuration going from d^0 to d^2. The shift of charge occurs in the highest occupied orbital (HOMO) for this series, which is based on the $3a_1$ orbital. Iso-surfaces for the HOMO of **Ia** and **Ic** are given in Fig. 4. In the transition state, both the hydride and the σ-bonded dihydrogen lie on the nodal plane of the $d(x^2)$-like HOMO. The increase in inter-ring angle along the exchange pathway found for **I** can be understood in terms of the need to stabilise the two electrons in the $3a_1$ orbital. The increased ease of forming the transition state with increase in inter-ring angle may also be due in part to the increase in stability of this orbital on bending.

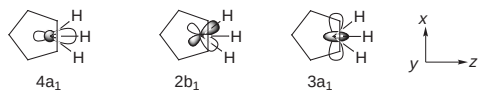

Fig. 3 Frontier orbitals for a bent metallocene unit.

Conclusions

The barrier width and height for hydrogen exchange in the tungstenocene trihydride cations has been shown to decrease with increase in inter-ring angle in a manner consistent with the magnitude of quantum mechanical exchange coupling found for these compounds. The origin of the effect can be traced to the changes in the metallocene frontier orbitals on bending the metallocene fragment. Two of the metal d orbitals become more involved in metal-ring bonding and are less available for binding the hydrogens. The binding to the central hydrogen is particularly affected and is very weak. In the carbon-bridged compound this leads to an (η²–H_2)H structure lying around 7 kJ mol^{-1} above the ground state. A third d orbital, which is non-bonding with respect to the cyclopentadienyl rings, is stabilised on bending and its lower energy favours formation of the d^2 transition state.

Finally, we wish to comment on an apparent paradox. Elimination of methane from d^2 *ansa*-bridged systems is less favoured than from unbridged systems,[37] yet the studies reported here show that in the *ansa*-bridged systems ligands appear to be less strongly bound. The paradox may be resolved by recognising that different factors are responsible in each

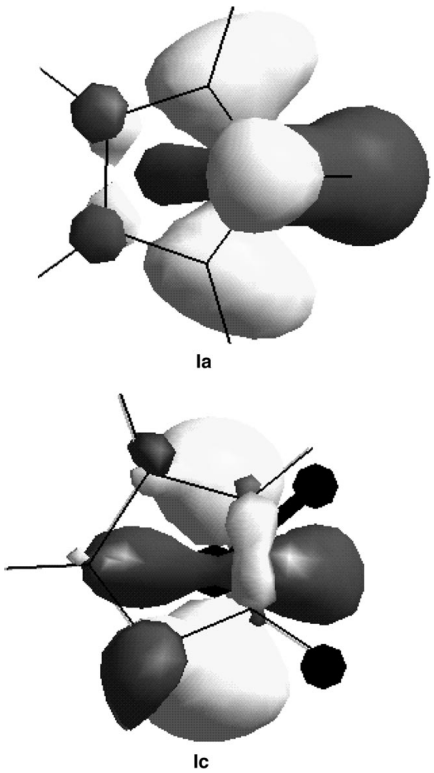

Fig. 4 Iso-surfaces for the HOMO along the exchange pathway of **Ia** and **Ic**, showing the shift of electron density to the metal along the exchange pathway.

case. In an elimination reaction an intermediate is formed with two more d electrons. These are most stable in a triplet, parallel ring structure. The presence of the bridge prevents access to such a geometry. Effective breaking of the metal ligand bonds does not represent the maximum energy on the reaction coordinate; rather it is the decomposition of an intermediate σ-complex and the loss of the product, such as methane, which is the real barrier. *Ansa*-bridges are thus seen to enable intramolecular exchange processes while simultaneously retaining ligands.

Acknowledgements

We thank Christian Jardine, Malcolm Green and Adam Stephens for valuable discussions. This work was carried out in part using computational resources of a DEC 8400 multiprocessor cluster (Columbus/Magellan), provided by the U.K. Computational Chemistry Facility at Rutherford Appleton Laboratory (admin.: Department of Chemistry, King's College London, Strand, London WC2R 2LS).

References

1 R. Paciello and J. E. Bercaw, *Abstracts of the 191st Meeting of the American Chemical Society*, American Chemical Society, Washington, DC, 1986, INOR 82.
2 T. Arliguie, B. Chaudret, J. Devillers and R. Poilblanc, *C. R. Séances Acad. Sci., Ser. II*, 1987, **305**, 1523.
3 A. Antiñolo, B. Chaudret, G. Commenges, M. Fajardo, F. Jalon, R. H. Morris, A. Otero and C. T. Schweltzer, *J. Chem. Soc., Chem. Commun.*, 1988, 1210.
4 D. M. Heinekey, N. G. Payne and G. K. Schulte, *J. Am. Chem. Soc.*, 1988, **110**, 3088.
5 S. Sabo-Etienne and B. Chaudret, *Chem. Rev.*, 1998, **98**, 2077 and references therein.
6 K. W. Zilm, D. M. Heinekey, J. M. Millar, N. G. Payne and P. J. Demou, *J. Am. Chem. Soc.*, 1989, **111**, 3088.
7 D. M. Heinekey, N. G. Payne and C. D. Sofield, *Organometallics*, 1990, **9**, 2643.
8 K. W. Zilm, D. M. Heinekey, J. M. Millar, N. G. Payne, S. P. Neshyba, J. C. Duchamp and J. Szczyrba, *J. Am. Chem. Soc.*, 1990, **112**, 920.
9 D. H. Jones, J. A. Labinger and D. P. Weitekamp, *J. Am. Chem. Soc.*, 1989, **111**, 3087.
10 H. H. Limbach, G. Scherer, M. Maurer and B. Chaudret, *Angew. Chem., Int. Ed. Engl.*, 1992, **31**, 1369.
11 E. Clot, C. Leforestier, O. Eisenstein and M. Pélissier, *J. Am. Chem. Soc.*, 1995, **117**, 1797.
12 J. Eckert and G. J. Kubas, *J. Phys. Chem.*, 1993, **97**, 2378.
13 E. M. Hiller and R. A. Harris, *J. Chem. Phys.*, 1993, **98**, 2077.
14 E. M. Hiller and R. A. Harris, *J. Chem. Phys.*, 1993, **99**, 7652.
15 E. M. Hiller and R. A. Harris, *J. Chem. Phys.*, 1994, **100**, 2522.
16 S. Szymanski, *J. Chem. Phys.*, 1996, **104**, 8216.
17 C. Scheurer, R. Wiedenbruch, R. Meyer, R. R. Ernst and D. M. Heinekey, *J. Chem. Phys.*, 1997, **106**, 1.
18 D. M. Heinekey, A. S. Hinkle and J. D. Close, *J. Am. Chem. Soc.*, 1996, **118**, 5353.
19 H. H. Limbach, S. Ulrich, S. Gründemann, G. Buntkowsky, S. Sabo-Etienne, B. Chaudret, G. J. Kubas and J. Eckert, *J. Am. Chem. Soc.*, 1998, **120**, 7929.
20 M. D. Curtis, L. G. Bell and W. M. Butler, *Organometallics*, 1985, **4**, 701.
21 D. M. Heinekey, *J. Am. Chem. Soc.*, 1991, **113**, 6074.
22 A. Chernega, J. Cook, M. L. H. Green, L. Labella, S. J. Simpson, J. Souter and A. H. H. Stephens, *J. Chem. Soc., Dalton Trans.*, 1997, 3225.
23 S. L. J. Conway, T. Dijkstra, L. H. Doerrer, J. C. Green, M. L. H. Green and A. H. H. Stephens, *J. Chem. Soc., Dalton Trans.*, 1998, 2689.
24 U. Drexler, R. Wiedenbruch, C. Scheurer, R. Meyer, R. R. Ernst, S. Chaloupka and L. M. Venanzi, *Mol. Phys.*, 1998, **93**, 471.
25 J. F. LeBoeuf, O. Lavastre, J. C. Leblanc and C. Moïse, *J. Organomet. Chem.*, 1986, **418**, 359.
26 S. Sabo-Etienne, B. Chaudret, H. Abou El-Makarim, J. C. Barthelat, J. P. Daudey, S. Ulrich, H. H. Limbach and C. Moïse, *J. Am. Chem. Soc.*, 1995, **117**, 11602.
27 F. A. Jalon, A. Otero, B. Manzano, E. Villasenor and B. Chaudret, *J. Am. Chem. Soc.*, 1995, **117**, 10123.
28 T. Arliguie, C. Border, B. Chaudret, J. Devillers and R. Poilblanc, *Organometallics*, 1989, **8**, 1308.
29 S. Gründemann, H. H. Limbach, V. Rodriguez, B. Donnadieu, S. Sabo-Etienne and B. Chaudret, *Ber. Bunsenges. Phys. Chem.*, 1998, **102**, 344.
30 R. G. Bergman and T. M. Gilbert, *J. Am. Chem. Soc.*, 1985, **107**, 3506.
31 D. M. Heinekey, J. M. Millar, T. F. Koetzle, N. G. Payne and K. W. Zilm, *J. Am. Chem. Soc.*, 1990, **112**, 909.
32 D. M. Heinekey and T. G. P. Harper, *Organometallics*, 1991, **10**, 2891.
33 D. G. Gusev, R. Kuhlman, G. Sini, O. Eisenstein and K. G. Caulton, *J. Am. Chem. Soc.*, 1994, **116**, 2685.
34 A. Castillo, M. A. Esteruelas and N. Ruiz, *J. Am. Chem. Soc.*, 1997, **119**, 9691.
35 R. Kuhlman, E. Clot, C. Leforestier, W. E. Sreib, O. Eisenstein and K. G. Caulton, *J. Am. Chem. Soc.*, 1997, **119**, 10153.
36 J. C. Green, *Chem. Soc. Rev.*, 1998, **27**, 263.
37 J. C. Green and C. N. Jardine, *J. Chem. Soc., Dalton Trans.*, 1998, 1057.
38 S. Camanyes, F. Maseras, M. Moreno, A. Llèdos, J. M. Lluch and J. Bertràn, *J. Am. Chem. Soc.*, 1996, **118**, 4617.
39 A. Jarid, M. Moreno, A. Llèdos, J. M. Lluch and J. Bertràn, *J. Am. Chem. Soc.*, 1993, **115**, 5861.
40 A. Jarid, M. Moreno, A. Llèdos, J. M. Lluch and J. Bertràn, *J. Am. Chem. Soc.*, 1995, **117**, 1069.
41 A. Antiñolo, F. Carillo-Hermosilla, M. Fajardo, S. Garcia-Yuste, A. Otero, S. Camanyes, F. Maseras, M. Moreno, A. Llèdos and J. M. Lluch, *J. Am. Chem. Soc.*, 1997, **119**, 6107.
42 S. Camanyes, F. Maseras, M. Moreno, A. Llèdos, J. M. Lluch and J. Bertràn, *Inorg. Chem.*, 1998, **37**, 2334.
43 G. te Velde and E. J. Baerends, *J. Chem. Phys.*, 1992, **99**, 84.
44 S. H. Vosko, L. Wilk and M. Nusair, *Can. J. Phys.*, 1980, **58**, 1200.
45 A. D. Becke, *Phys. Rev. A*, 1988, **38**, 2398.
46 J. P. Perdew, *Phys. Rev. B*, 1986, **34**, 7046.
47 J. P. Perdew, *Phys. Rev. B*, 1986, **33**, 8822.
48 R. D. Wilson, T. F. Koetzle, D. W. Hart, A. Kvick, D. L. Tipton and R. Ball, *J. Am. Chem. Soc.*, 1977, **99**, 1775.

Paper 9/01341E